Mechanistic understanding of crystal violet dye sorption by woody biochar: implications for wastewater treatment

Awanthi Wathukarage · Indika Herath · M. C. M. Iqbal · Meththika Vithanage

Abstract Dye-based industries, particularly small and medium scale, discharge their effluents into waterways without treatment due to cost considerations. We investigated the use of biochars produced from the woody tree *Gliricidia sepium* at 300 °C (GBC300) and 500 °C (GBC500) in the laboratory and at 700 °C from a dendro bioenergy industry (GBC700), to evaluate their potential for sorption of crystal violet (CV) dye. Experiments were conducted to assess the effect of pH reaction time and CV loading on the adsorption process. The equilibrium adsorption capacity was higher with GBC700 (7.9 mg g^{-1}) than GBC500 (4.9 mg g^{-1}) and GBC300 (4.4 mg g^{-1}), at pH 8. The CV sorption process was dependent on the pH, surface area and pore volume of biochar (GBC). Both Freundlich and Hill isotherm models fitted best to the equilibrium isotherm data suggesting cooperative interactions via physisorption and chemisorption mechanisms for CV sorption. The highest Hill sorption capacity of 125.5 mg g^{-1} was given by GBC700 at pH 8. Kinetic data followed the pseudo-second-order model, suggesting that the sorption process is more inclined toward the chemisorption mechanism. Pore diffusion, π–π electron donor–acceptor interaction and H-bonding were postulated to be involved in physisorption, whereas electrostatic interactions of protonated amine group of CV and negatively charged GBC surface led to a chemisorption type of adsorption. Overall, GBC produced as a by-product of the dendro industry could be a promising remedy for CV removal from an aqueous environment.

A. Wathukarage · M. C. M. Iqbal (✉)
Plant and Environmental Sciences, National Institute of Fundamental Studies, Kandy, Sri Lanka
e-mail: mcmif2003@yahoo.com

A. Wathukarage
Postgraduate Institute of Science, University of Peradeniya, Peradeniya, Sri Lanka

I. Herath · M. Vithanage
Environmental Chemodynamics Project, National Institute of Fundamental Studies, Kandy, Sri Lanka

M. Vithanage (✉)
Faculty of Applied Sciences, University of Sri Jayewardenepura, Nugegoda 10250, Sri Lanka
e-mail: meththika@sjp.ac.lk

Keywords Chemisorption · Physisorption · Cationic dyes · Wastewater treatment · Crystal violet · Gliricidia

Introduction

Synthetic dyes are extremely stable due to their complex aromatic compounds. They are considered to have disease causing properties such as carcinogenic, mutagenic, teratogenic and allergic actions on

living organisms (Yagub et al. 2014). Basically, 30% of the world production of dyes may be lost during the dyeing process and the effluents can consist of up to 10–50 mg L^{-1} of dye concentration (Nethaji and Sivasamy 2011). It has been estimated that 10–20% of triarylmethane dyes from the dyeing process are released to the natural water surface without pre-treatment (Schoonen and Schoonen 2014). Crystal violet (CV) is one of the most commonly used synthetic, cationic dyes, belongs to the triarylmethane group and is widely used in textile dyeing, biological staining and paintings. In addition, CV is also used as a pH indicator, external disinfectant (Mittal et al. 2010), dermatological agent and veterinary medicine (Guzel et al. 2014).

Cationic dyes are highly toxic with respect to anionic dyes, and their trinctorial values are very high (<1 mg L^{-1}) (Guzel et al. 2014). Accordingly, CV has high color intensity and is highly visible in aqueous solutions even in low concentrations, which can lead to severe color pollution. In aquatic ecosystems, the color prevents sunlight penetration through the water column resulting in a decline in the primary production besides health effects on aquatic fauna and flora (Hameed and Ahmad 2009). Removal of CV dye from industrial effluent is therefore essential prior to their disposal to ensure the protection of the environment and human health. Generally, CV is classified as carcinogenic and is a recalcitrant molecule due to its non-biodegradability and can be persistent in a variety of environments (Saeed et al. 2010). Hence, it may tend to traverse through the food chains, leading to bioaccumulation and biomagnification in wildlife and humans (Guzel et al. 2014). Furthermore, CV dye causes skin, respiratory and digestive tract irritations (Zhang et al. 2014) and even in extreme cases as respiratory ailments, kidney failures and permanent blindness (Mittal et al. 2010). Thus, the remediation of CV effluents prior to their disposal is an emerging concern in addressing environmental and water pollution.

For dye removal from aqueous systems, methods such as flocculation, coagulation, membrane filtration, chemical oxidation, ion exchange, electrolysis and reverse osmosis have been used (Yagub et al. 2014; Rafatullah et al. 2010). However, they are inefficient and ineffective as the dyes are complex and fairly highly soluble in aqueous medium (Mittal et al. 2010) with high stability and recalcitrant nature toward light,

aerobic digestion and oxidizing agents (Demirbas 2009). Adsorption is a widely used technique world-wide, due to its simplicity, cost-effectiveness and easy operation without producing harmful by-products (Feng et al. 2013) and also can be used for a wide variety of dyes and for large-scale dye removal (Ghaedi et al. 2013). Several studies have shown that the activated carbon derived from different materials such as coconut fiber (Demirbas 2009), and coconut pith (Nethaji and Sivasamy 2011) can be successfully applied for the removal of methylene blue from aqueous solutions. However, the use of activated carbon is not worthwhile due to its high cost (Alshabanat et al. 2013). Hence, finding alternatives for activated carbon is necessary for a sustainable solution for dye removal from aqueous systems.

Biochar is recognized as a sustainable alternative for activated carbon for removing a wide spectrum of pollutants from soil and aqueous systems (Vithanage et al. 2016, 2017). While biochar has been used as a soil amendment in the recent past to improve crop yield and soil fertility, researchers have now explored the possibility of using it as a biosorbent to isolate environmental pollutants (Tan et al. 2015; Vithanage et al. 2014). Biochar is economically and environmentally beneficial due to less energy requirement, carbon negative production and recycling of organic waste materials, through the pyrolysis process (Ahmad et al. 2013). The temperature of pyrolysis and the type of biomaterial are crucial parameters in terms of biochar properties for sorption capacity (Ahmad et al. 2014). Pyrolysis of organic waste wood is an effective strategy in terms of energy production. Through this process, biochar and ash would be the possible by-products and this biochar can be used directly for remediation purposes (Lucchini et al. 2014). Although, several adsorbents have been used to study CV sorption such as organic waste products, grapefruit peel, wheat bran, coniferous pinus (Yagub et al. 2014), industrial by-products; bottom ash, de-oiled soya (Mittal et al. 2010) and inorganic materials; kaolin (Yagub et al. 2014), few studies have reported on dye removal using biochar derived from different materials such as water hyacinth (Xu et al. 2016), kenaf fiber (Mahmoud et al. 2012), cellulose, coconut shell, groundnut shell, rice husk and straw (Kannan and Sundaram 2001; Kulkarni et al. 2017; Zhou et al. 2014). Magnetized biochar showed significant improvement of the adsorption capacity of CV even

more than activated carbon (349 mg g^{-1}) (Sun et al. 2015; Yakout and Ali 2015). *Gliricidia sepium* derived biochar, obtained from a bioenergy industry as a by-product, has recently been applied for the remediation of heavy metals in contaminated-soils and pesticides in water (Herath et al. 2015; Bandara et al. 2015; Mayakaduwa et al. 2015). Nevertheless, this woody biochar has not been tested for its potential for removing dyes from wastewater.

Hence, investigating the potential of removal of cationic dyes by using waste by-products could be a crucial strategy for wastewater treatment while addressing the waste management problem in bioenergy industries. The primary objective of this study is to provide a cost-effective solution for small dye industries to effectively remove CV from their effluent before discharging into public waterways. The sorption characteristics of biochar from *Gliricidia sepium* (GBC) produced at different pyrolysis temperatures and a bioenergy industry-derived GBC for CV removal were evaluated and compared using equilibrium and kinetic mechanistic modeling.

Materials and methods

Chemicals

Crystal violet, CI 42555, IUPAC name Tris(4-(dimethylamino)phenyl)methylium chloride (Fig. S1) was purchased from Sigma-Aldrich (99% purity). A stock solution of 1000 mg L^{-1} was prepared in distilled water. Successive dilutions from the stock solution were used to prepare the experimental solution of relevant concentrations for batch sorption studies, and each experiment was carried out with fresh dilutions. Nitric acid (0.1 M HNO$_3$) and sodium hydroxide 0.1 M NaOH were used for adjusting the pH of the dye solution. All reagents were of analytical grade.

Biochar production and characterization

Biochar was produced from the biomass of a woody tree, *Gliricidia sepium*, provided by a dendro thermal power plant in Thirappane, Sri Lanka. The wood was cut into small pieces, crushed and oven-dried at 60 °C for 24 h. Dried biomass was pyrolyzed in closed crucibles at 300, and 500 °C under limited O$_2$ supply by using a Muffle Furnace (model P330, Nabertherm,

Germany). Pyrolysis heating rate was adjusted to 7 °C min^{-1} for 3 h to obtain a slow pyrolysis process (Ahmad et al. 2013). GBC derived at 700 °C was collected directly from the dendro thermal power plant. Powdered GBC was cooled to room temperature and sieved to <1 mm particle size. GBC pyrolyzed at 300, 500 °C and the dendro bioenergy industry-derived biochar at 700 °C were denoted as GBC300, GBC500 and GBC700 for the experiments, respectively. The pH and EC were measured by using pH meter and electrical conductivity meter in 1:10 suspensions of biochar to water. Surface area was determined by using BET method, while pore volumes and pore diameter were measured through BJH (Barrett-Joyner-Halenda) method. Elemental analysis was conducted by using an elemental analyzer (Vario MAX CN, elementar, Hanau, Germany). FTIR spectra were collected in the range of 400–4000 cm^{-1} by a Nicolet FTIR spectrophotometer (Model 6700, USA) to detect surface functional groups of the biochar and dye loaded biochar. In addition, quantification of functional groups in biochar was determined by using modified Boehm titration experiment (Fidel et al. 2013).

Batch sorption studies

The factors that affect the sorption process such as pH, initial dye concentration and contact time were studied for pyrolyzed GBC through batch experiments. Experiments were carried out in 50 mL tubes with 25 mL of CV solution; the tubes were equilibrated in the linear shaker at room temperature at 120 rpm. The pH range was 3–9, and initial dye concentration was 5–200 mg L^{-1}. The biochar dose of 2 g L^{-1} and equilibrium time of 4 h were used for all sorption experiments based on the preliminary dosage and kinetic studies. After shaking for the required time duration the samples were micro-centrifuged at 7000 rpm for 10 min. The supernatant was analyzed by a UV–VIS spectrometer (UV-160A Shimadzu, Japan) at 590 nm wave length to determine the residual dye concentration (Sun et al. 2015).

Isotherm studies

Adsorption isotherms were carried out for the three types of GBCs in different CV concentrations at pH 8, keeping the temperature constant (30 °C). Dye

solutions of 25 mL with different concentrations (5–200 mg L^{-1}) were used by adding an adsorbent dose of 2 g L^{-1} and equilibrated. These tubes were taken out, centrifuged and analyzed.

The amount of dye adsorption q_e (mg g^{-1}) was calculated by Eq. (1).

$$q_t = [C_0 - C_e]V/M \qquad (1)$$

where q_e is the solid-phase dye equilibrium concentration (mg g^{-1}), C_0 and C_e are the initial and equilibrium dye concentrations (mg L^{-1}), respectively, V is the solution volume (L), and M is the mass of biochar (g).

Equilibrium isotherm models of Langmuir, Freundlich, Temkin, Dubinin–Radushkevich and Hill were used to describe dye adsorption onto GBC300, GBC500 and GBC700. The equations of Langmuir and Freundlich, Temkin, Dubinin–Radushkevich and Hill models are expressed, by Eqs. (2), (3), (5),(6) (Rajapaksha et al. 2015) and (7) (Foo and Hameed 2010).

Langmuir isotherm (Eq. 2) refers to homogeneous adsorption and assumes that all sites of the adsorbent possess a uniform affinity for the adsorbate. In contrast the Freundlich isotherm model (Eq. 3) suggests multilayer adsorption, with non-uniform affinities over the heterogeneous surface of the adsorbent.

$$q_{ads} = \frac{q_{max}K_L C_e}{1 + K_L C_e} \qquad (2)$$

$$q_{ads} = K_F C_e^{1/n} \qquad (3)$$

where q_e is the amount of dye adsorbed per unit weight of biochar (mg g^{-1}), C_e is the equilibrium dye concentration (mg L^{-1}). q_{max} is the maximum adsorption capacity, and K_L refers to the Langmuir affinity parameter related to the energy adsorption. K_F and n are Freundlich constants; K_F indicates the bond strength, while n indicates the bond energies between the dye and the biochar.

The separation factor (R_L), which is based on Langmuir parameters, is used to determine whether the sorption of dye onto biochar was favorable or unfavorable in batch experiments and is expressed by Eq. 4:

$$R_L = \frac{1}{1 + K_L C_o} \qquad (4)$$

The Temkin isotherm model Eq. (5) refers to the heat of sorption which assumes that the adsorption energy decreases linearly with the surface coverage and the bonding energy implies a uniform distribution up to a certain maximum energy.

$$q_{ads} = \frac{RT}{b}\ln(AC_e) \qquad (5)$$

where R is the universal gas constant (8.314 J K^{-1} mol^{-1}), T is the absolute temperature, b is the heat of adsorption, and A is the binding constant (L mg^{-1}).

The Dubinin–Radushkevich Eq. (6) model refers to the multilayer adsorption mechanism with Van der Waals forces.

$$q_{ads} = q_D \exp(-B_D[RT\ln(1 + 1/C_e)]^2 \qquad (6)$$

where q_D is the adsorption capacity (mg g^{-1}) and B_D is the mean free energy of sorption.

Hill isotherm model Eq. (7) assumes that the adsorption capacity is a cooperative phenomenon and describes the binding of different molecules onto homogeneous substrates.

$$q_{ads} = \frac{q_{s_H}C_e^{n_H}}{K_D + C_e^{n_H}} \qquad (7)$$

where K_D is the Hill constant, n_H is the Hill cooperativity coefficient of the binding interaction, and q_{SH} refers to the Hill isotherm maximum uptake saturation (mg L^{-1}).

Kinetic studies

Kinetic study was conducted for GBC700 to investigate the effect of contact time on dye sorption. Adsorbent dosage, pH and initial dye concentration were kept constant and at their optimum value. Dye solution of 25 mL was used for each tube with an adsorbent dose of 2 g L^{-1} and equilibrated. The tubes were taken out at different time intervals (from 5 min–8 h), centrifuged and analyzed by the UV–Vis spectrophotometer at 590 nm wave length. The amount of adsorption q_t (mg g^{-1}), at time t (min), was calculated by Eq. (8).

$$q_t = [C_0 - C_t]V/M \qquad (8)$$

where C_t is the concentration of the CV at time t (mg L^{-1}).

Kinetic models of pseudo-first-order, pseudo-second-order, Elovich and parabolic models were used to investigate the mechanism of dye sorption onto GBC700. The equations of pseudo-first-order, pseudo-second-order, Elovich and parabolic kinetic models are expressed as Eqs. (9), (10), (11) (Vithanage et al. 2016) and (12) (Zeng et al. 2004).

The pseudo-first-order kinetic model (Eq. 9) describes the reversibility of equilibrium between the liquid and solid phases.

$$q_t = q_e \left(1 - \exp^{-k_1 t}\right) \tag{9}$$

where q_e is the amount of dye adsorbed at $t = 0$ (mg g^{-1}), K_1 is the pseudo-first-order rate constant (min^{-1}).

The pseudo-second-order kinetic model Eq. (10) is related to the rate limiting of the chemical adsorption, which is expressed as:

$$q_t = \frac{K_2 q_e^2 t}{1 + K_2 q_e t} \tag{10}$$

where q_e is the amount of dye adsorbed at $t = 0$ (mg g^{-1}), K_2 is the pseudo-second-order rate constant (min^{-1}).

The Elovich kinetic model Eq. (11) is expressed as:

$$q_t = 1/\beta \ln(\alpha\beta) + (1/\beta) \ln t \tag{11}$$

The parabolic model Eq. (12) describes the diffusion-controlled phenomena which are rate limiting.

$$q_t = a + k_p t^{\frac{1}{2}} \tag{12}$$

where k_p is the diffusion rate constant ((cm^2 s^{-1}))$^{-0.5}$ and a is a constant.

Statistical analysis

All isotherm and kinetic parameters were determined by nonlinear regressions using Origin 6.0 software. The goodness of fit for the isotherm models was evaluated by comparing the coefficient of determination (r^2) and Chi-square (χ^2). The Chi-square (χ^2) values were calculated by using Eq. (13).

$$\chi^2 = \frac{\sum (q_{ex} - q_m)^2}{q_m} \tag{13}$$

where q_{ex} and q_m are the experimental and model calculated equilibrium capacity (mg g^{-1}), respectively.

Results and discussion

Biochar characterization

The properties of GBC varied with the temperature of pyrolysis. The pH of GBC increased with raising pyrolysis temperature (Table 1). This may be due to separation of alkali salts from Gliricidia and loss of acidic functional groups at higher pyrolysis temperature (Rajapaksha et al. 2015). Similarly, cation exchange capacity (CEC) of the biochars increased with the elevation of the pyrolysis temperature due to the concentration of Ca^{2+}, Mg^{2+}, Na$^+$ and K$^+$ elements without volatilizing through the pyrolysis process (Al-Wabel et al. 2013).

Lower molar ratio of O/C indicated the poor polarity nature of the GBC suggesting less hydrophilicity and high stability of the biochar surface (Ahmad et al. 2013), while lower polarity index (O+N)/C links with the reduction in surface polar functional groups (Rajapaksha et al. 2014). The molar O/C ratio and the polarity index (O+N)/C decreased with increasing pyrolysis temperature (Table 1). The

Table 1 Proximate analysis and ultimate analysis of Gliricidia biochar derived at 300 °C (GBC300), 500 °C (GBC500) and 700 °C (GBC700)

Sample	GBC300	GBC500	GBC700
pH	6.71	9.27	10.42
EC (μScm^{-1})	212.35	537.5	1703.50
Proximate analysis			
Moisture (%)	3.57	2.66	11.27
Mobile matter (%)	28.58	11.79	23.81
Resident matter (%)	61.80	70.80	44.40
Ash (%)	6.03	14.68	20.51
Yield (%)	39.58	26.24	–
Ultimate analysis			
C (%)	75.46	73.29	92.75
H (%)	4.76	3.55	1.46
O (%)	24.35	19.0	2.80
N (%)	0.72	0.84	0.73
Molar H/C	0.06	0.05	0.02
Molar O/C	0.32	0.26	0.03
Molar (O+N)/C	0.33	0.27	0.04
Surface area (m^2 g^{-1})	1.02	76.30	808.00
Pore volume (cm^3 g^{-1})	0.001	0.010	0.890

molar O/C reduced from 0.32 at GBC300 to 0.25 at GBC500 and 0.03 at GBC700, and polarity index (O+N)/C reduced from 0.33 at GBC300 to 0.27 at GBC500 and 0.04 at GBC700. GBCs became more hydrophobic with the increase in pyrolysis temperature. Removal of acidic functional groups during the pyrolysis process leads to enhanced basicity of biochar surface, with the elevation of the pyrolysis temperature (Ahmad et al. 2013).

Molar H/C ratio implies the aromaticity, and H/C ratio less than 0.1 indicates graphite-like structures (Ahmad et al. 2013). Molar ratios of GBC700, GBC500 and GBC300 were reduced to 0.06, 0.05 and 0.02, respectively. Lower molar H/C values of GBC indicated that the GBC derived under the higher pyrolysis temperature consisted of highly carbonized aromatic structures (Rajapaksha et al. 2014). The aromatic structure of the surface of GBC700 was further confirmed by the FTIR spectral data. Thus, it can be confirmed that GBC700 is highly stable with respect to the GBC500 and GBC300.

Surface area and pore properties of GBC also changed with the pyrolysis temperature (Table 1). A drastic increment of surface area of GBC700 (808.00 m^2 g^{-1}) was observed relative to GBC500 (76.30 m^2 g^{-1}) and GBC300 (1.02 m^2 g^{-1}). Lower surface area at low pyrolysis temperature (<700 °C) is attributed to the formation of tar components during the pyrolysis process which prevents the formation or hinders the continuity of pores (Rajapaksha et al. 2015). In contrast, these tar components may volatilize at higher pyrolysis temperature (>700 °C) under a huge pressure and enhance the biochar surface area (Ahmad et al. 2013). Similar results have been reported in several previous studies, where they have revealed that higher surface area often resulted at higher pyrolysis temperature (700–750 °C) (Ahmad et al. 2013). Similar to the surface area, the pore volume was also increased with the elevation of pyrolysis temperature and GBC700 showed the highest value of 0.89 cm^3 g^{-1}. However, pore diameters were recorded as 38.40 nm at GBC300, 70.30 nm at GBC500 and 4.08 nm at GBC700. These results revealed that GBC300 and GBC700 dominate with mesopores (2–50 nm), while GBC500 dominates with macro pores (>50 nm).

Scanning electron microscopic (SEM) images (Fig. S2) showed the amorphous and heterogeneous structures of GBC relative to their biomass. The occurrence and development of channels, macro-, meso- and micropores were well observed in GBC700 compared to the GBC500 and GBC300. Formation of these vesicles may be due to the release of volatile components under an extensive internal pressure at high pyrolysis temperatures resulting in combination of smaller pores, enlargements of internal cavities and the splitting into amorphous structures (Rajapaksha et al. 2014).

FTIR characterization

The FTIR spectra of the GBC300, GBC500, GBC700 and the CV loaded GBC700 are shown in Fig. S3. There is a significant decrease in the peaks of the following functional groups with increasing pyrolysis temperature: –OH stretching of hydrogen bonding, –CH_2 stretching of polar groups and C=O and C=C stretching of lignin, phenolic –OH and C–O–C stretching of cellulose. Pyrolysis of the Gliricidia biomass results in a dehydration of the cellulose and ligneous content, and condensation of the aromatic units. The spectrum of GBC700 shows peaks at 875, 1090, 1429 and 3437 cm^{-1}. The small peak at 875 cm^{-1} is attributed to the aromatic –CH out of plane bending (Rajapaksha et al. 2015) due to the condensation of the small aromatic units into larger sheets, an indication of the highly aromatic nature of GBC700. The broad peak at 1090 cm^{-1} can be attributed to phenolic OH (Vithanage et al. 2016) or Si–O stretching vibrations, and peak 1429 cm^{-1} represents the CO_3^{2-} stretching frequencies (carbonate) group (Herath et al. 2015). Further, quantitation of functionalities within the GBC700 by Boehm titration depicts the presence of acidic like lactonic, phenolic and carboxylic groups in biochar, respectively, 297.61, 402.86 and 34.07 µmol g^{-1}, while the 743.55 µmol g^{-1} of total acidic groups represents within the adsorbent. Moreover, representation of basic groups was quite high for GBC700 and quantitatively 2017.67 µmol g^{-1} present in the sample. The peak at 3437 cm^{-1} of raw GBC700 is assigned to the phenolic –O–H stretch. After the adsorption of CV, the new peaks appeared at 1171, 1366 and 1586 cm^{-1} corresponding to secondary amine C–N stretch (Coates 2000), aromatic tertiary amine C–N stretch (Kant et al. 2014) and –NH (Sun et al. 2015) group, respectively. This confirms the adsorption of CV by these functional groups in GBC700.

Adsorption studies

Effect of pH

The sorption of CV onto the three GBCs was highly pH dependent. The variation in the amount of CV adsorbed by the three GBCs with the initial pH of the solution is shown in Fig. 1a. The equilibrium adsorption capacity of GBC700 (7.9 mg g^{-1}) was twice as much as that of GBC500 (4.9 mg g^{-1}) and 300 (4.4 mg g^{-1}), at pH > 7 and therefore GBC700 showed the highest equilibrium sorption capacity compared to GBC500 and GBC300. With increasing pH of the solution, the sorption of CV onto GBC700 increased significantly from 5.4 mg g^{-1} at pH 3 to 7.9 mg g^{-1} at pH 9 with equilibrium occurrence at pH > 7 (Fig. 1a). The optimum pH for maximum sorption of CV (7.9 mg g^{-1}) was observed at an average of pH 8. Thus, the sorption of CV onto all GBCs is highly pH dependent since it affects the surface charge of the adsorbent. In addition, the interaction of the ionic and functional surface group can influence the adsorption process. Being a cationic dye, CV would be preferably adsorbed onto a biosorbent surface with a negative charge (El Saliby et al. 2013). At low pH values (pH = 2) the high concentration of H$^+$ ions and its smaller ionic radius would give them a competitive advantage over the larger CV molecules, resulting in reduced adsorption of CV molecules (Sun et al. 2015). The adsorption capacity of the adsorbent is further reduced by the repulsion between the protonated adsorbent and the CV molecules (Zhou et al. 2014). Similar observation to our study was made by Sun et al. (2015) with corn stalk biochar magnetized with Fe$_3$O$_4$, where optimum pH was 6.0 (Table 4).

The point of zero charge (pHpzc) of the GBC700 further explains the role of pH in the CV adsorption process. The pHpzc of the GBC700 was 7.4 (Fig. 1b). When the solution pH is below the pHpzc, the surface of the adsorbent is positively charged and it becomes negative if the pH is above the pHpzc (Mohsen Nourouzi et al. 2010). In this study, the maximum sorption occurred at 8 pH, which is above the pHpzc (pH > 7.4). At this point, the surface of biochar becomes negatively charged, exhibiting predominantly strong electrostatic interactions with positively charged CV molecules, since the CV dye is dissociated as C$_{25}$H$_{30}$N$_3^+$ and Cl$^-$ in aqueous medium. At higher pH (pH > 7), this cationic form of CV is highly stable, thereby resulting in a maximum sorption. With further increase in the solution pH, the available binding sites on the biochar surface are progressively saturated leading to a constant CV adsorption. The least CV sorption was observed at pH < 7 due to electrostatic repulsive forces of positively charged biochar surface and the cationic CV molecule. Studies have also shown that cationic dye adsorption is more favored at pH > pHpzc due to the presence of OH$^-$, COO$^-$ functional groups on the adsorbent surface (Sahmoune and Yeddou 2016).
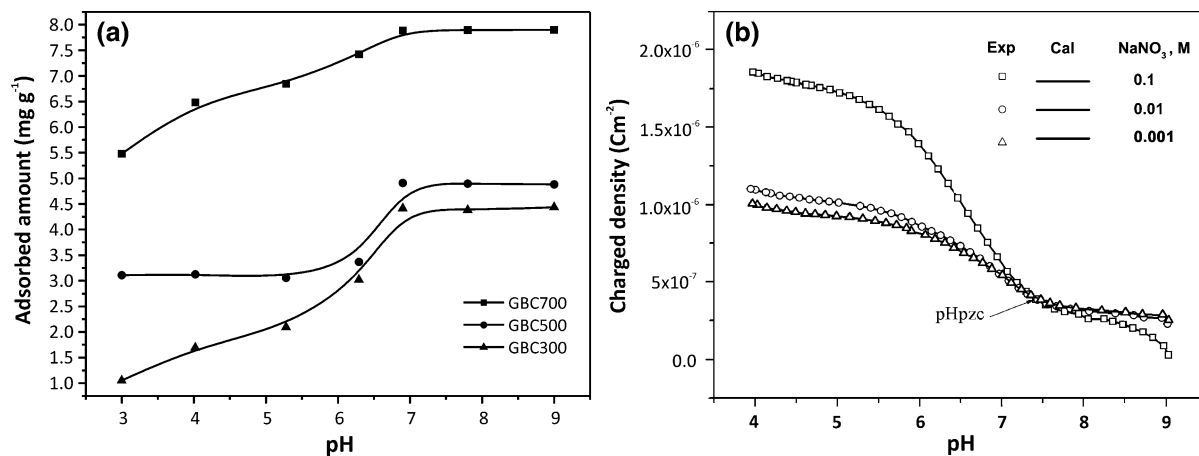

Fig. 1 a Effect of solution pH on the sorption of crystal violet dye for Gliricidia biochar derived at 300 °C (GBC300), 500 °C (GBC500) and 700 °C (GBC700). b Variations of surface charge with pH based on the three different ionic strengths. Gliricidia biochar derived at 700 °C (GBC700) concentration = 0.5 g L^{-1}, pHpzc = 7.4

Isotherm studies

Adsorption isotherm models generally describe the relationship between the amount of CV adsorbed by a unit weight of adsorbent and the remaining amount of substance in the solution at equilibrium. The adsorption amount of the CV increased with the increase of initial dye concentration for all three types of GBCs. The driving force of adsorption depends on the solute concentration gradient between the adsorbent and the adsorbate (Song et al. 2011). At low concentrations, the adsorption of CV was much difficult due to the lower concentration gradient of dye ions between the biochar and the solution. In contrast, higher dye concentrations enhanced the dye removal process through increasing the driving force, which retards the resistance toward the dye adsorption until the saturation of all the active sites on the biochar surface is achieved (Mahmoud et al.

2012). In GBC700, the amount of dye adsorbed per unit mass increased from 0.9 to 25 mg g^{-1}. In contrast, the amount of dye adsorbed per unit mass increased from 1.8 to 14 mg g^{-1} with GBC500 and 1 to 8.9 mg g^{-1} for GBC300, respectively.

To understand the isotherm behaviors of CV adsorption, onto GBC, the data were fitted to the models of Langmuir, Freundlich, Temkin, Dubinin–Radushkevich and Hill. The values for the parameters of nonlinear adsorption isotherm models fitted for all the biochars at pH 8 are summarized in Table 2. The Freundlich and Hill isotherms fitted well for all the biochars tested in this study with respect to the Langmuir, Temkin and Dubinin–Radushkevich isotherm models according to the regression coefficient (r^2) and Chi-square (χ^2) values (Table 2). The adsorption isotherm models fitted for GBC700 are shown in Fig. 2a. The Freundlich isotherm can be applied to

Table 2 Freundlich and Hill isotherm parameters for crystal violet dye adsorption onto Gliricidia biochar derived at 300 °C (GBC300), 500 °C (GBC500) and 700 °C (GBC700) at pH 8

Isotherms										
Adsorbent	Freundlich				Hill					
	r^2	χ^2	K_F (mg g^{-1})	$1/n$	r^2	χ^2	q_{SH} (mg g^{-1})	K_D	n_H
GBC300	0.9314	0.623	0.68	0.66	0.9477	0.631	11.02	0.0500	1.50
GBC500	0.9037	3.759	1.49	0.54	0.9013	3.853	23.71	0.0242	0.95
GBC700	0.9746	2.790	5.86	0.38	0.9747	3.338	125.53	0.0009	0.43

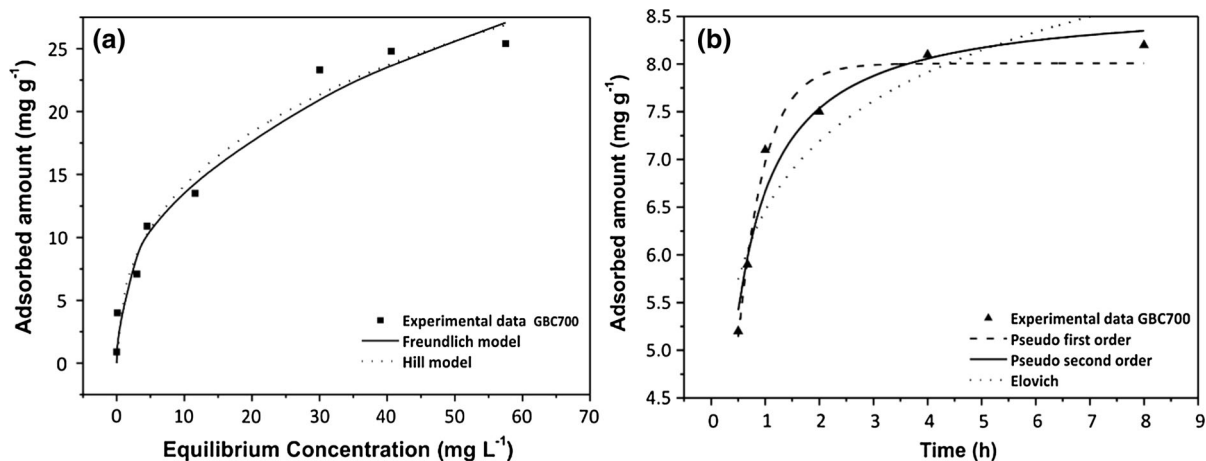All parameters were calculated by nonlinear regression

Fig. 2 **a** Adsorption isotherm fitting of biochar at 700 °C (GBC700) to Freundlich model and Hill model at pH 8. **b** Adsorption kinetic fitting of biochar produced at 700 °C (GBC700) to pseudo-second-order, pseudo-first-order and Elovich model
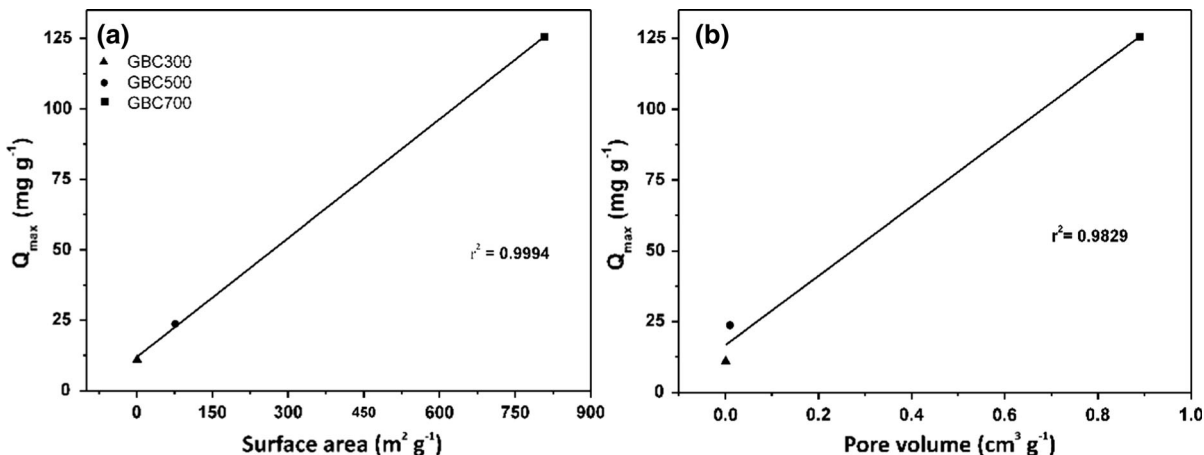
Fig. 3 Correlation among Hill adsorption capacity Q_{max} and **a** surface area and **b** pore volume for Gliricidia biochar derived at 300 °C (GBC300), 500 °C (GBC500) and 700 °C (GBC700). The linear regression is represented by the *lines*

multilayer adsorption with non-uniform distribution of adsorption heat and affinities over the heterogeneous surface (Foo and Hameed 2010). The experimental data fitted to the Freundlich isotherm model indicated that the adsorption process is more inclined toward physisorption type interactions. The Freundlich constant (K_f) expresses the degree of adsorption; an increase in K_f values with increasing pyrolysis temperature suggests that the adsorption process is highly favorable in biochars produced at high pyrolysis temperatures (Chakraborty 2011). Thus, the results suggest that GBC700 has the highest adsorption capacity for CV adsorption compared to GBC300 and GBC500. The term 1/n is considered as a measure of the adsorption intensity, and the deviation of 1/n from 1 indicated a greater heterogeneity of the biochar surface (Vithanage et al. 2014). All the n values lay between 1 and 10, and therefore, 1/n values were lower than 1. This indicates a favorable adsorption of CV by all three types of biochars. The availability of new binding sites for the adsorption process from a greater surface heterogeneity of the sorbent increased the adsorption capacity. The value of 1/n significantly decreased with increasing pyrolysis temperature of the GBC, and the least 1/n value of GBC700 further confirmed the feasibility of the adsorption process on GBC700. Biochars derived at high temperatures have given high capacities for adsorbing organic pollutants such as deisoprpyla-trazine, trichloroethylene and carbofuran, etc. (Mahtab Ahmad et al. 2014).

The Hill isotherm model indicates the existence of possible cooperative interactions via chemical bonding between the CV molecules and the biochar surface. The model illustrates when a ligand is capable of binding with a macromolecule; it can also influence the binding ability of other ligands onto the same macromolecule (Foo and Hameed 2010). Hence, cooperative interactions can occur on the surface of the biochar creating strong chemical bonding between the functional groups present on the biochar surface and more than one group of the CV molecules. The Hill cooperativity coefficient (n_H) provides a way to quantify this effect, and $n_H > 1$ indicates a positive cooperativity (Vithanage et al. 2014), whereas $n < 1$ indicates negative cooperativity. Maximum sorption capacities (q_{SH}) of CV were obtained through the Hill equation with the values of GBC700 (125.53 mg g^{-1}) > GBC500 (23.71 mg g^{-1}) > GBC300 (11.02 mg g^{-1}). GBC700 showed the highest sorption capacity resulting in a relatively greater adsorption of CV. This adsorption capacity was twice as much as the Langmuir adsorption capacity of a nonporous carbon derived from tomato paste (68.97 mg g^{-1}) for the removal of CV from aqueous solution (Guzel et al. 2014).

Kinetic studies

The highest sorption capacity from the edge and isotherm experiments was shown by GBC700. Kinetic study was conducted only for GBC700 in order to

Kinetics

Pseudo-first-order					Pseudo-second-order				Elovich			
q_e, exp (mg g^{-1})	q_e, cal (mg g^{-1})	K_1 (min^{-1})	r^2	χ^2	q_e, cal (mg g^{-1})	K_2 (g mg^{-1} min^{-1})	r^2	χ^2	q_e, cal (mg g^{-1})	K_2 (mg kg^{-1})$^{-5}$	r^2	χ^2
9.24	9.21	1.0	0.6160	0.884	9.17	0.3	0.9703	0.068	9.50	5.2	0.8586	0.260

All parameters were calculated by nonlinear regression

study the kinetic behavior and thereby postulate further sorption mechanisms of CV onto GBC700. The removal of CV increased with the time of contact with GBC700 and equilibration was observed after 4 h. The rate of dye removal was initially rapid with 7.5 mg g^{-1} of CV adsorbed within 2 h; thereafter, it gradually declined attaining equilibrium after 4 h at 8.1 ± 0.6 mg g^{-1} (Fig. 2b). Hence, the adsorption kinetics showed a two-stage sorption process: an initial rapid phase followed by a slow phase. This can be attributed to the availability of vacant sites on the biochar at the initial stages, which are rapidly occupied by the CV molecules followed by a slowing down of the sorption process as less sites are available, and reaching an equilibrium stage when all the available sites are saturated. This was similar to the conclusions made in previous studies on methylene blue adsorption onto modified biochar derived from Water hyacinth (Xu et al. 2016).

The kinetic models fitted for GBC700 are shown in Fig. 3, and the estimated values for kinetic model parameters are given in Table 3. Based on the highest regression coefficient (r^2) and lowest Chi-squares (χ^2), the pseudo-second-order kinetic model provided a satisfactory fit for the adsorption kinetics of CV onto GBC700. Predicted adsorption capacity value (qe cal = 9.17) from the pseudo-second-order model matched well with the experimental adsorption capacity value (qe exp = 9.24), which further confirmed the goodness of the fitting of experimental data to the pseudo-second-order model. Fitting experimental data to pseudo-second-order kinetic model suggests that chemical sorption may have occurred by involving the valency forces through sharing or exchange of electrons between the sorbent and the sorbate and hence chemisorption may be the rate limiting step (Chakraborty 2011). Thus, this may further confirm the involvement of chemisorption interactions between surface of GBC700 and CV dye molecules.

Possible mechanisms for CV dye adsorption

In this study, the mechanistic modeling of kinetic and isotherm data indicated that both physisorption and chemisorption mechanisms govern the adsorption of CV by GBC700. Hence, the mechanisms of adsorption onto GBC700 can be explained by the complexation of CV dye via physical and chemical interactions (Fig. 4). Physical adsorption occurs by the forces of
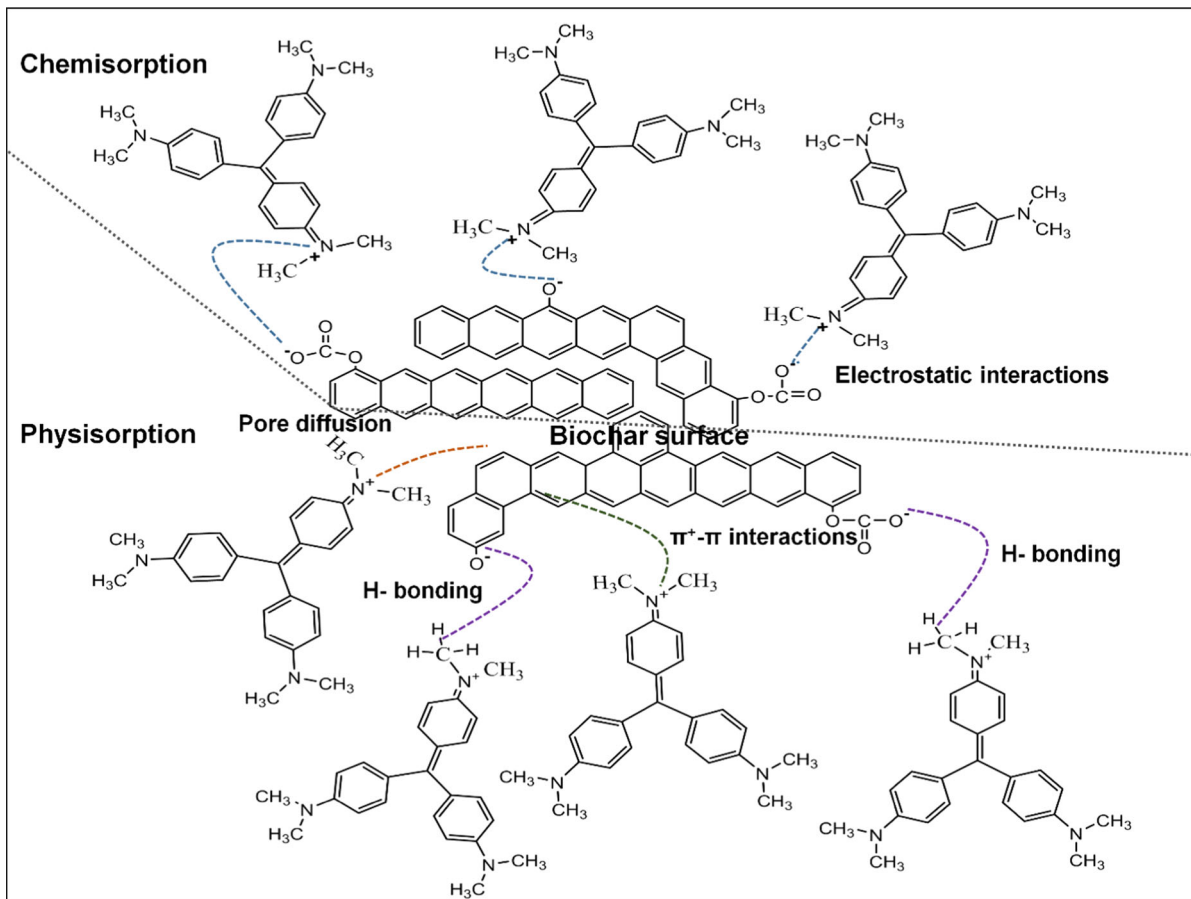
Fig. 4 Graphical representation of possible crystal violet dye adsorption mechanisms onto Gliricidia biochar derived at 700 °C (GBC700)

molecular interactions including van der Waals dispersion forces, $\pi^+-\pi$ electron donor–acceptor interactions and hydrogen bonding via H-donor acceptor interactions (Nidheesh et al. 2012). These forces on the surface of the biochar are created from physical changes such as surface area, pore volume and surface functional groups. On the other hand, chemisorption mainly takes place through electrostatic interactions between the negatively charged biochar surface and positively charged CV molecule, thereby leading to a strong CV adsorption on the biochar surface. The graphical representation of possible CV adsorption mechanism onto GBC700 is illustrated in Fig. 4.

The high pyrolysis temperature can induce physical changes on the GBC surface such as surface area and pore volume (M. Ahmad et al. 2014). Relatively, GBC700 showed significant changes in surface area and pore volume, which enhances the sorption capacity

through the diffusion of CV into the GBC pores. Pore diffusion would be the primary mechanism of CV sorption onto GBC produced at higher pyrolysis temperatures. This is proven by the correlation tests performed against the Hill maximum adsorption capacity versus the surface area and pore volume (Fig. 3) for all the three types of biochar. A positive correlation was observed between the Hill adsorption capacity and surface area ($r^2 = 0.9994$), indicating that the surface area is a key parameter of biochar for the sorption of CV dye. Similarly, correlation test against the pore volume of the biochars showed a positive correlation ($r^2 = 0.9829$) with the Hill adsorption capacity. This is also supported by the pore data of GBC700 which consists of more mesopores (2–50 nm) than micropores (0–2 nm) and macropores (>50 nm) relative to GBC500 and GBC300. The molecular size of the CV dye molecule is 1.4 nm × 1.4 nm (Guzel

Table 4 Comparison of crystal violet adsorption by several adsorbents

Adsorbent	Dosage (g L^{-1})	Initial Conc. of CV (mg L^{-1})	Contact time (min)	Solution temperature (°C)	Optimum (pH)	Maximum adsorption capacity (mg g^{-1})	References
Coniferous pinus bark powder	2.0	10–50	120	30	8.0	32.78	Ahmad (2009)
Grapefruit peel	–	10–600	60	30	6.0	254.16	Saeed et al. (2010)
NaOH-modified rice husk	10.0	50	90	20	8.0	44.87	Chakraborty (2011)
Magnetic nanocomposite	1.0	240–400	135	50	8.5	113.13	Singh et al. (2011)
TiO$_2$-based nanosheet	1.0	10–100	–	–	8.5	56.30	Chen et al. (2012a, 2012b)
Palm kernel fiber	2.0	20–160	60	25	8.0	78.90	El-Sayed (2011)
CarAlg/MMt nanocomposite hydrogels	1.0	10–100	120	–	6.4	88.80	Mahdavinia et al. (2013)
Nano-porous carbon from tomato waste	2.0	25–200	150	50	8.0	68.97	Guzel et al. (2014)
Cellulose	1.0	50–200	150	20	9.0	112.00	Zhou et al. (2014)
Cellulose-based adsorbent	1.0	50–200	150	20	9.0	182.15	Zhou et al. (2014)
Fe$_3$O$_4$-coated biochar	1.0	100–500	240	40	6.0	349.90	Sun et al. (2015)
GBC700 (by-product)	2.0	5–200	240	30	8.0	125.53	This study
GBC500	2.0	5–200	240	30	8.0	23.71	This study
GBC300	2.0	5–200	240	30	8.0	11.02	This study

et al. 2014). Thus, the diffusion of CV molecules into meso- and macropores is possible. In addition, hydrophobic interactions can occur between the non-polar long-chain graphene structure of the biochar surface and less polar aromatic groups of the CV molecule. The new peak at 1586 cm^{-1} in CV adsorbed GBC700 (Fig. S3) may be due to NH-stretching (Sun et al. 2015), or aromatic C=C stretching in the adsorbed CV molecule (Guzel et al. 2014) that confirms the adsorption of CV onto GBC700 surface.

The π^{+}–π electron donor–acceptor interaction is considered as another specific mechanism for CV adsorption on the GBC. It is evident that the organocations that has amine groups can act as π electron acceptors and involve with the formation of π^{+}–π electron donor–acceptor interactions with the π electron-rich polyaromatic surface of pyrogenic carbonaceous materials such as biochar, black carbon and

graphene. Hence, the electron-rich graphene surface of the GBC can bind with the protonated amino group of the CV molecule forming strong π^{+}–π electron donor–acceptor interactions. Here, the graphene sites act as the electron donor, while CV dye cations act as the electron acceptor. This newly formed C–N bond stretching frequency corresponds to the new peak that appeared at 1171 cm^{-1} in the FTIR spectrum of CV-treated GBC 700 (Fig. S3). Similar observations are reported in adsorption of carbofuran in acidic medium on to biochar derived with rice husk and tea waste through π^{+}–π electron donor–acceptor interactions (Vithanage et al. 2016). Moreover, strong H-bonding can occur at H-donor and acceptor groups present on the biochar surface and the CV molecule. This may occur through involving the methane groups in CV molecules and the phenolic, alcohol and carbonate groups presence in biochar surface. The formation of

such intermolecular H-bonding is evident with the appearance of significantly increased O–H stretching frequencies at 3437 cm^{-1}, with a decline in the stretching vibration of phenolic O–H at 1090 cm^{-1} in the FTIR spectrum of CV adsorbed GBC700. Adsorption through H-donor and acceptor groups present on the biochar surface and cationic adsorbents corroborates the previous findings (Vithanage et al. 2016).

Chemisorption can take place through electrostatic forces between the negatively charged biochar surface and positively charged CV molecule. The biochar surface tends to be negatively charged at higher pH (pH > 7) due to phenolate and carbonate anions which enhances the electrostatic attraction of the positively charged cationic CV molecule (Ahmad et al. 2014). Existence of such chemisorption interactions is evident with the FTIR spectral data. Boehm evidences support to prove the presence and their protonation of phenolic and lactonic groups. The peak at 1429 cm^{-1} in untreated GBC700 corresponds to the CO_3^{2-} stretching vibration, and this band clearly shifted to 1366 cm^{-1} in CV-treated GBC700. Furthermore, phenolic O–H stretching frequencies at 1090 cm^{-1} diminished in the CV adsorbed GBC700 spectrum. These changes in bond frequencies of CO_3^{2-} and phenolic OH groups could possibly be due to the formation of strong chemical bonding between the CV molecules. Electrostatic attraction of the positively charged cationic dyes onto the negatively charged biochar surface corroborates the finding of (Xu et al. 2011) with the proposed mechanism.

Conclusions

The present study was conducted to evaluate the effects of different temperature-derived Gliricidia biochars for the removal of crystal violet dye in aqueous solution. Gliricidia biochar obtained from the bioenergy industry (GBC700) had higher surface area (808.00 m^2 g^{-1}) and pore sizes (0.890 cm^3 g^{-1}) relative to the biochar produced at 500 °C (76.30 m^2 g^{-1}, 0.010 cm^3 g^{-1}) and 300 °C (1.02 m^2 g^{-1}, 0.001 cm^3 g^{-1}). Biochar properties changed significantly with the pyrolysis temperature. The surface area ($r^2 = 0.9994$) and pore volume ($r^2 = 0.9829$) of all three biochars correlated positively with the Hill adsorption capacity values,

confirming significant involvement of surface area and pore size on the sorption of CV. GBC700 (7.9 mg L^{-1}) showed the highest equilibrium sorption capacity compared to GBC500 (4.9 mg g^{-1}) and GBC300 (4.4 mg g^{-1}) at pH 8 through the edge experiments. Both Freundlich and Hill isotherm models fitted best with the equilibrium isotherm data suggesting cooperative-type interactions via physisorption and chemisorption mechanisms which govern the CV sorption process. The kinetics of the sorption process was explained well by the pseudo-second-order model, indicating that the CV adsorption onto GBC would be more inclined toward chemisorption-type interactions. Pore diffusion, π–π electron donor–acceptor interaction and H-bonding were postulated to be involved in physisorption, whereas electrostatic interactions led to chemisorption type of adsorption. From the overall results, it can be concluded that Gliricidia biochars produced at higher temperatures are highly effective in removing CV from aqueous solutions.

References

Ahmad, R. (2009). Studies on adsorption of crystal violet dye from aqueous solution onto coniferous pinus bark powder (CPBP). *Journal of Hazardous Materials, 171*(1), 767–773.

Ahmad, M., Lee, S. S., Rajapaksha, A. U., Vithanage, M., Zhang, M., Cho, J. S., et al. (2013). Trichloroethylene adsorption by pine needle biochars produced at various pyrolysis temperatures. *Bioresource Technology, 143*, 615–622.

Ahmad, M., Rajapaksha, A. U., Lim, J. E., Zhang, M., Bolan, N., Mohan, D., et al. (2014a). Biochar as a sorbent for contaminant management in soil and water: A review. *Chemosphere, 99*, 19–33.

Ahmad, M., Vithanage, M., Koutsospyros, A., Lee, S. S., Yang, J. E., et al. (2014b). Production and use of biochar from buffalo-weed (*Ambrosia trifida* L.) for trichloroethylene removal from water. *Journal of Chemical Technology and Biotechnology, 89*(1), 150–157.

Alshabanat, M., Alsenani, G., & Almufarij, R. (2013). Removal of crystal violet dye from aqueous solutions onto date palm fiber by adsorption technique. *Journal of Chemistry, 2013*, 6. doi:10.1155/2013/210239.

Al-Wabel, M., Al-Omran, A., El-Naggar, A. H., Nadeem, M., & Usman, A. R. (2013). Pyrolysis temperature induced changes in characteristics and chemical composition of biochar produced from conocarpus wastes. *Bioresource Technology, 131*, 374–379.

Bandara, T., Herath, I., Kumarathilaka, P., Seneviratne, M., Seneviratne, G., Rajakaruna, N., Vithanage, M., & Ok, Y. S. (2015). Role of woody biochar and fungal-bacterial

co-inoculation on enzyme activity and metal immobilization in serpentine soil. *Journal of Soils and Sediments*, *17*(3), 665–673.

Chakraborty, S. (2011). Adsorption of crystal violet from aqueous solution onto NaOH-modified rice husk. *Carbohydrate Polymers, 86,* 1533–1541.

Chen, F., Fang, P., Gao, Y., Liu, Z., Liu, Y., & Dai, Y. (2012a). Effective removal of high-chroma crystal violet over TiO$_2$-based nanosheet by adsorption–photocatalytic degradation. *Chemical Engineering Journal, 204–206,* 107–113. doi:10.1016/j.cej.2012.07.030.

Chen, F., Fang, P., Gao, Y., Liu, Z., Liu, Y., & Dai, Y. (2012b). Effective removal of high-chroma crystal violet over TiO$_2$-based nanosheet by adsorption–photocatalytic degradation. *Chemical Engineering Journal, 204,* 107–113.

Coates, J. (2000). Interpretation of infrared spectra, a practical approach. In R. A. Meyers (Ed.), *Encyclopedia of analytical chemistry* (pp. 10815–10837). Chichester: Wiley.

Demirbas, A. (2009). Agricultural based activated carbons for the removal of dyes from aqueous solutions: A review. *Journal of Hazardous Materials, 167,* 1–9.

El Saliby, I., Erdei, L., Kim, J. H., & Shon, H. K. (2013). Adsorption and photocatalytic degradation of methylene blue over hydrogen–titanate nanofibres produced by a peroxide method. *Water Research, 47*(12), 4115–4125.

El-Sayed, G. O. (2011). Removal of methylene blue and crystal violet from aqueous solutions by palm kernel fiber. *Desalination*, *272*(1), 225–232.

Feng, Y., Dionysiou, D. D., Wu, Y., Zhou, H., Xue, L., He, S., et al. (2013). Adsorption of dyestuff from aqueous solutions through oxalic acid-modified swede rape straw: Adsorption process and disposal methodology of depleted bioadsorbents. *Bioresource Technology, 138,* 191–197.

Fidel, R. B., Laird, D. A., & Thompson, M. L. (2013). Evaluation of modified Boehm titration methods for use with biochars. *Journal of Environmental Quality, 42*(6), 1771–1778.

Foo, K., & Hameed, B. H. (2010). Insights into the modeling of adsorption isotherm systems. *Chemical Engineering Journal, 156*(1), 2–10.

Ghaedi, M., Nasab, G. A., Khodadoust, S., Rajabi M., & Azizian, S. (2013). Application of activated carbon as adsorbents for efficient removal of methylene blue: Kinetics and equilibrium study. *Journal of Industrial and Engineering Chemistry*, *20*(4), 2317–2324.

Guzel, F., Saygılı, H., Saygılı, G. A., & Koyuncu, F. (2014). Decolorisation of aqueous crystal violet solution by a new nanoporous carbon: Equilibrium and kinetic approach. *Journal of Industrial and Engineering Chemistry, 20,* 3375–3386.

Hameed, B. H., & Ahmad, A. A. (2009). Batch adsorption of methylene blue from aqueous solution by garlic peel, an agricultural waste biomass. *Journal of Hazardous Materials, 164,* 870–875.

Herath, I., Kumarathilaka, P., Navaratne, A., Rajakaruna, N., & Vithanage, M. (2015). Immobilization and phytotoxicity reduction of heavy metals in serpentine soil using biochar. *Journal of Soils and Sediments, 15*(1), 126–138.

Kannan, N., & Sundaram, M. M. (2001). Kinetics and mechanism of removal of methylene blue by adsorption on various carbons—a comparative study. *Dyes and Pigments, 51*(1), 25–40.

Kant, A., Gaijon, P., & Nadeem, U. (2014). Adsorption equilibrium and kinetics of crystal violet dye from aqueous media onto waste material. *Chemical Science Review and Letters*, *3*(11S), 1–13.

Kulkarni, M. R., Revanth, T., Acharya, A., & Bhat, P. (2017). Removal of crystal violet dye from aqueous solution using water hyacinth: Equilibrium, kinetics and thermodynamics study. *Resource-Efficient Technologies, 3*(1), 71–77. doi:10.1016/j.reffit.2017.01.009.

Lucchini, P., Quilliam, R. S., Deluca, T. H., Vamerali, T., & Jones, D. L. (2014). Increased bioavailability of metals in two contrasting agricultural soils treated with waste wood-derived biochar and ash. *Environmental Science and Pollution Research, 21*(5), 3230–3240.

Mahdavinia, G. R., Aghaie, H., Sheykhloie, H., Vardini, M. T., & Etemadi, H. (2013). Synthesis of CarAlg/MMt nanocomposite hydrogels and adsorption of cationic crystal violet. *Carbohydrate Polymers*, *98*(1), 358–365.

Mahmoud, D. K., Salleh, M. A. M., Karim, W. A., Idris, A., & Abidin, Z. Z. (2012). Batch adsorption of basic dye using acid treated kenaf fibre char: equilibrium, kinetic and thermodynamic studies. *Chemical Engineering Journal, 181,* 449–457.

Mayakaduwa, S. S., Kumarathilaka, P., Herath, I., Ahmad, M., Al-Wabel, M., Ok, Y. S., et al. (2015). Equilibrium and kinetic mechanisms of woody biochar on aqueous glyphosate removal. *Chemosphere, 144,* 2516–2521.

Mittal, A., Mittal, J., Malviya, A., Kaur, D., & Gupta, V. K. (2010). Adsorption of hazardous dye crystal violet from wastewater by waste materials. *Journal of Colloid and Interface Science, 343,* 463–473.

Mohsen Nourouzi, M., Chuah, T. G., & Choong, T. S. (2010). Adsorption of glyphosate onto activated carbon derived from waste newspaper. *Desalination and Water Treatment, 24*(1–3), 321–326.

Nethaji, S., & Sivasamy, A. (2011). Adsorptive removal of an acid dye by lignocellulosic waste biomass activated carbon: Equilibrium and kinetic studies. *Chemosphere, 82*(10), 1367–1372.

Rafatullah, M., Sulaiman, O., Hashim, R., & Ahmad, A. (2010). Adsorption of methylene blue on low-cost adsorbents: A review. *Journal of Hazardous Materials, 177,* 70–80.

Rajapaksha, A. U., Vithanage, M., Ahmad, M., Seo, D. C., Cho, J. S., Lee, S. E., et al. (2015). Enhanced sulfamethazine removal by steam-activated invasive plant-derived biochar. *Journal of Hazardous Materials, 290,* 43–50.

Rajapaksha, A. U., Vithanage, M., Zhang, M., Ahmad, M., Mohan, D., Chang, S. X., et al. (2014). Pyrolysis condition affected sulfamethazine sorption by tea waste biochars. *Bioresource Technology, 166,* 303–308.

Saeed, A., Sharif, M., & Iqbal, M. (2010). Application potential of grapefruit peel as dye sorbent: Kinetics, equilibrium and mechanism of crystal violet adsorption. *Journal of Hazardous Materials, 179,* 564–572.

Sahmoune, M. N., Yeddou, A. R. (2016). Potential of sawdust materials for the removal of dyes and heavy metals: examination of isotherms and kinetics. *Desalination and Water Treatment*, *57*(50), 24019–24034.

Schoonen, M. A., & Schoonen, J. M. T. (2014). Removal of crystal violet from aqueous solutions using coal. *Journal of Colloid and Interface Science, 422,* 1–8.

Singh, K. P., Gupta, S., Singh, A. K., & Sinha, S. (2011). Optimizing adsorption of crystal violet dye from water by magnetic nanocomposite using response surface modeling approach. *Journal of Hazardous Materials*, *186*(2), 1462–1473.

Song, J., Zou, W., Bian, Y., Su, F., & Han, R. (2011). Adsorption characteristics of methylene blue by peanut husk in batch and column modes. *Desalination, 265,* 119–125.

Sun, P., Hui, C., Khan, R. A., Du, J., Zhang, Q., & Zhao, Y. H. (2015). Efficient removal of crystal violet using Fe_3O_4-coated biochar: The role of the Fe_3O_4 nanoparticles and modeling study their adsorption behavior. *Scientific Reports, 5,* 12638. doi:10.1038/srep12638.

Tan, X., Liu, Y., Zeng, G., Wang, X., Hu, X., Gu, Y., et al. (2015). Application of biochar for the removal of pollutants from aqueous solutions. *Chemosphere, 125,* 70–85.

Veetil Nidheesh, P., Gandhimathi, R., Thanga Ramesh, S., & Anantha Singh, T. S. (2012). Adsorption and desorption characteristics of crystal violet in bottom ash column. *Journal of Urban and Environmental Engineering, 6*(1), 18–29.

Vithanage, M., Herath, I., Joseph, S., Bundschuh, J., Bolan, N., Ok, Y. S., Kirkham, M. B., & Rinklebe, J. (2017). Interaction of arsenic with biochar in soil and water: A critical review. *Carbon*, *113*, 219–230.

Vithanage, M., Mayakaduwa, S. S., Herath, I., Ok, Y. S., & Mohan, D. (2016). Kinetics, thermodynamics and mechanistic studies of carbofuran removal using biochars from tea waste and rice husks. *Chemosphere*, *150*, 781–789.

Vithanage, M., Rajapaksha, A. U., Tang, X., Thiele-Bruhn, S., Kim, K. H., Lee, S. E., et al. (2014). Sorption and transport of sulfamethazine in agricultural soils amended with invasive-plant-derived biochar. *Journal of Environmental Management, 141,* 95–103.

Xu, R. K., Xiao, S. C., Yuan, J. H., & Zhao, A. Z. (2011). Adsorption of methyl violet from aqueous solutions by the biochars derived from crop residues. *Bioresource Technology, 102*(22), 10293–10298.

Xu, Y., Liu, Y., Liu, S., Tan, X., Zeng, G., Zeng, W., Ding, Y., Cao, W., & Zheng, B. (2016). Enhanced adsorption of methylene blue by citric acid modification of biochar derived from water hyacinth (Eichornia crassipes). *Environmental Science and Pollution Research*, *23*(23), 23606–23618.

Yagub, M. T., Sen, T. K., Afroze, S., & Ang, H. M. (2014). Dye and its removal from aqueous solution by adsorption: A review. *Advances in Colloid and Interface Science, 209,* 172–184.

Yakout, S. M., & Ali, M. S. (2015). Removal of the hazardous crystal violet dye by adsorption on corncob-based and phosphoric acid-activated carbon. *Particulate Science and Technology, 33*(6), 621–625. doi:10.1080/02726351.2015.1016642.

Zeng, L., Li, X., & Liu, J. (2004). Adsorptive removal of phosphate from aqueous solutions using iron oxide tailings. *Water Research, 38*(5), 1318–1326.

Zhang, Q., Zhang, T., He, T., & Chen, L. (2014). Removal of crystal violet by clay/PNIPAm nanocomposite hydrogels with various clay contents. *Applied Clay Science, 90,* 1–5.

Zhou, Y., Zhang, M., Wang, X., Huang, Q., Min, Y., Ma, T., et al. (2014). Removal of crystal violet by a novel cellulose-based adsorbent: Comparison with native cellulose. *Industrial and Engineering Chemistry Research, 53*(13), 5498–5506.